

Cellular delivery of antibodies: effective targeted subcellular imaging and new therapeutic tool

Marzia Massignani ^{a,b,‡}, Irene Canton ^{a,‡}, Nisa Patikarnmonthon ^a, Nicholas J. Warren ^{a,c}, Steven P. Armes ^c, Andrew L. Lewis ^d, Giuseppe Battaglia ^{a*}

^aThe Krebs Institute, Department of Biomedical Science, University of Sheffield, Firth Court, Sheffield, S10 2TN, United Kingdom

^bBiomaterials and Tissue Engineering Group, Department of Engineering Materials, University of Sheffield, North Campus, Broad Lane, Sheffield, S3 7HQ, United Kingdom

^cDepartment of Chemistry, University of Sheffield, Brook Hill, Sheffield, S3 7HF, United Kingdom

^dBiocompatibles UK Ltd., Farnham Business Park, Weydon Lane, Farnham, United Kingdom

[‡]these authors have contributed to the work equally

* corresponding author: Dr G. Battaglia, The Krebs Institute, Department of Biomedical Science, University of Sheffield, Firth Court, Western Bank, Sheffield, S10 2TN, United Kingdom, Tel:+44 114 2222305 email:

g.battaglia@sheffield.ac.uk

Abstract

It is already more than a century since the pioneering work of the Nobel Laureate Ehrlich gave birth to the side chain theory^{1, 2} which helped to define antibodies and their ability to target specific biological sites. However, the use of antibodies is still restricted to the extracellular space due to the lack of a suitable delivery vehicle for the efficient transport of antibodies into live cells without inducing toxicity. In this work, we report the efficient encapsulation and delivery of antibodies into live cells with no significant loss of cell viability or any deleterious effect on the cell metabolic activity. This delivery system is based on poly(2-(methacryloyloxy)ethyl phosphorylcholine)-block-(2-(diisopropylamino)ethyl methacrylate), (PMPC-PDPA), a pH-sensitive diblock copolymer³ that self-assembles to form nanometer-sized vesicles, also known as polymersomes,⁴ at physiological pH. These polymersomes can successfully deliver relatively high antibody payloads within live cells. Once inside the cells, we demonstrate that these antibodies can target their epitope by immune-labelling of cytoskeleton, Golgi, and transcription factor proteins in live cells. We also demonstrate that this effective antibody delivery mechanism can be

used to control specific subcellular events, as well as modulate cell activity and pro-inflammatory process.

There is an emerging need in both pharmacology and within the biomedical industry to develop new tools to investigate intracellular mechanisms, since a greater understanding of such processes should ultimately provide innovative therapeutics. The efficient delivery of functionally active proteins within cells is a potentially powerful research strategy, especially for intracellular antibodies⁵. Nevertheless, the available methodologies for intracellular delivery are often restricted by adverse effects on the protein function and stability, mainly due to the extensive **chemical** modifications that are normally required for such approaches⁶. Recent strategies for the intracellular delivery of functional proteins include the use of liposomes to encapsulate both proteins and genes for intracellular delivery⁷, antibody delivery via protein transduction domains (PTD)⁸, membrane receptors and transport signals⁹⁻¹¹, viral vectors¹², microinjection¹³ or electroporation¹⁴. However, each of these methods lack convenience and effectiveness and moreover are often compromised by cellular toxicity¹⁵. Some of these limitations have been overcome by delivering transcriptionally-active DNA into cultured cells to express a desired protein, which then acts as an intracellular target¹⁶.

Herein we present a non-cytotoxic delivery system based on a pH-sensitive diblock copolymer that self-assembles at physiological pH to form nanometer-sized polymersomes. These polymersomes successfully deliver functional antibodies into the cytoplasm. More specifically, polymersomes were formed using a PMPC-PDPA diblock copolymer comprising a highly biocompatible poly(2-(methacryloyloxy)ethyl phosphorylcholine) (PMPC) block and a pH-sensitive poly(2-(diisopropylamino)ethyl methacrylate) (PDPA) block (with a pK_a of $\sim 5.8-6.6$, depending on the ionic strength)¹⁷. Polymersomes are uptaken by cells via endocytosis¹⁸ and hence experience a rapid drop in local pH. Under these conditions, the polymersomes dissociate rapidly to form individual copolymer chains. This causes a sudden increase (by several orders of magnitude) in the number of species that are present and the consequent osmotic shock ruptures the endosomal membrane. Cell internalization kinetics can be precisely tuned by careful control of polymersome size and surface topology¹⁸ and these polymersomes have been employed for the efficient intracellular delivery of plasmid DNA¹⁹ and various fluorophores.²⁰ Moreover, the presence of PMPC-PDPA polymersomes within cells consistently has a negligible effect on cell viability and stress levels over a broad range of cell types, including both primary cells and cell lines.^{18, 21, 22}

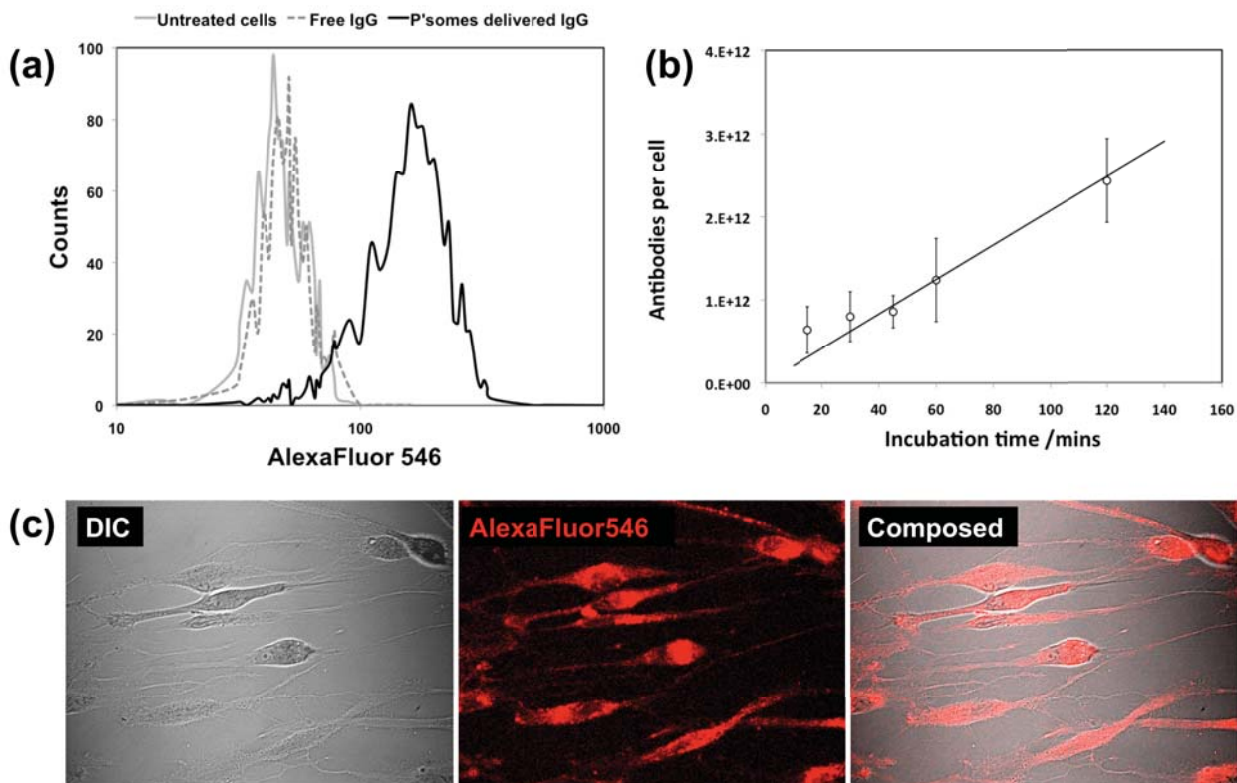


Figure 1. Effective delivery of an antibody within live cells. Confocal Laser Scanning Microscopy (CLSM) micrographs of live HDF cells recorded using DIC, red channel and ‘composed image’ modes after polymersome-mediated delivery of AlexaFluor546-IgG. (a) Fluorescence Activated Cell Sorting (FACS) of HDF cells after 2 h incubation with AlexaFluor546-IgG-loaded polymersomes (b). Quantification of antibody uptake as a function of incubation time (c).

Results

Cytosolic antibody delivery

In order to assess effective cytosolic delivery of antibody within live cells, we encapsulated AlexaFluor546-labelled IgG antibodies within PMPC-PDPA polymersomes, followed by incubation with primary live human dermal fibroblasts (HDF) for various time periods. The treated cells were subsequently washed thoroughly and analysed by confocal microscopy (Figure 1a), Fluorescence Activated Cell Sorting (FACS) (Figure 1b) and fluorescence spectroscopy after lyses (Figure 1c). Confocal Laser Scanning Microscopy (CLSM) revealed that the fluorescently-labelled antibodies were

delivered effectively within the cytosol, almost regardless of the cell type. This was also confirmed by FACS analysis, as shown in Figure 1b, where HDF cells treated with AlexaFluor546-labelled IgG loaded polymersomes were approximately an order of magnitude more fluorescent than either untreated control cells or cells treated with free antibody. The extent of antibody delivery was further assessed by incubating cells with polymersomes for different times and quantifying the amount of intracellular antibody present after cell lysis by uv-visible absorption spectroscopy. Cell internalization kinetic data (see Figure 1c) confirm that (i) uptake of antibody-loaded polymersomes is detectable within 30 minutes of incubation and (ii) the fluorescence intensity rapidly increases within the first 2 h of incubation time (N.B. Cells treated with free antibodies exhibited no fluorescence in control experiments). The increase in fluorescence intensity per cell can be attributed to the intracellular release of the AlexaFluor 546- IgG. These data are consistent with previous work from our group, which indicated that polymersome internalization increases linearly with time, despite cellular division.^{18, 21} Volumetric analysis of antibody distribution within the cells using CLSM allows precise imaging of cells at different focal planes. Live cells exhibit strong fluorescent signals from the cytosol (Figure S1a-b). These results were compared with a traditional immunolabelling method (Figure S1c-d) where permeabilised fixed cells were treated with the same concentration of antibody (AlexaFluor 546 goat Anti-mouse IgG).

The precise mechanism for the intracellular delivery of antibodies is not yet known. However, we have observed^{22, 23} that, in order to achieve efficient endocytosis, the polymersome surface chemistry (and hence the cell binding ability) is crucial in order to determine whether effective and fast endocytosis is achieved. We have demonstrated that polymersome entry is controlled by endocytosis and also identified some of the steps in the entry mechanism, such as acidification and microtubule-guided transportation.¹⁸ Although further work is needed to elucidate the uptake mechanism in more detail, we verified that endosome escape is definitely triggered by the pH-sensitive nature of the polymersomes.^{18, 21} To further validate the entry mechanism, and more importantly the endosome escape, we encapsulated 15 nm gold-labelled IgG antibodies within the polymersomes. HDF cells were treated for 24 h and subsequently analysed by transmission electron microscopy (TEM). The 15 nm gold was easily identifiable within the cells and only those cells treated with antibody-loaded polymersomes displayed gold-IgG within the cytosol (Figure S2). In Figure 2a a high magnification TEM micrograph clearly confirms this finding in more detail. All the various steps such as polymersome endocytosis, trafficking vesicle, endosomal escape and, more importantly, the delivered antibody within the cytosol (circled) can be observed. This confirms our hypothesis of endosomal membrane destabilisation and

subsequent delivery of the antibody within the cytosol. In Figure 2b, a detailed mechanism for polymersome-mediated antibody delivery is proposed, showing the various steps.

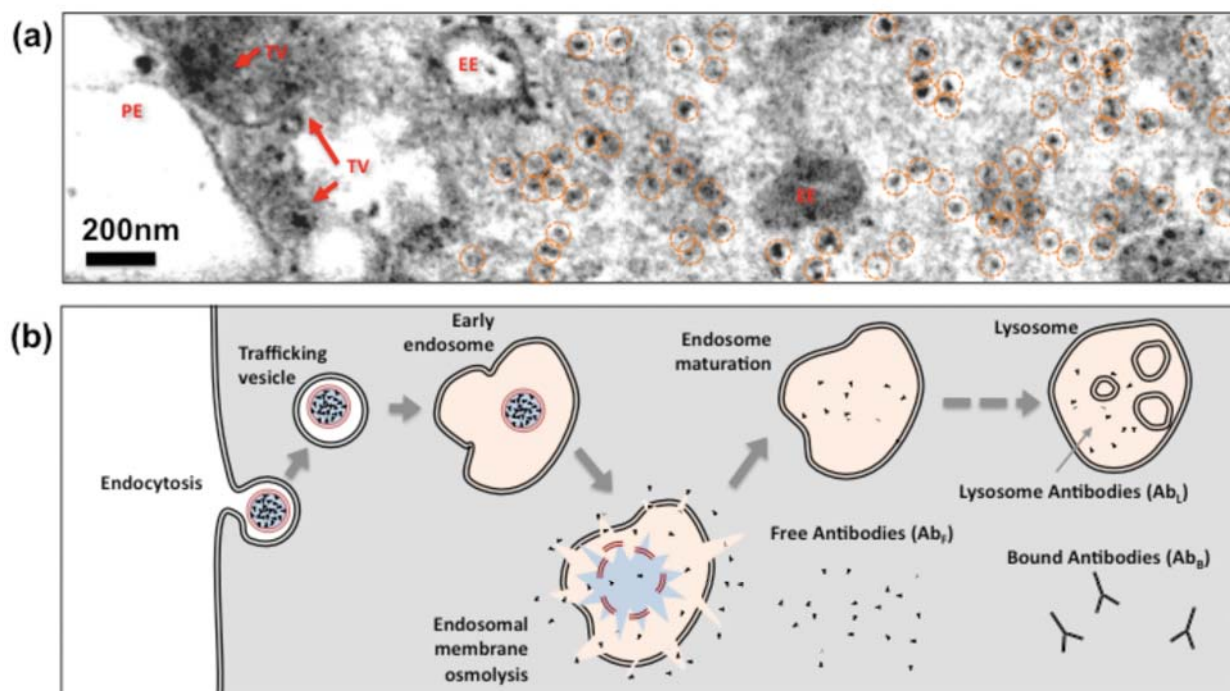


Figure. 2. Mechanism of cytosolic delivery of antibodies. TEM image obtained for a HDF cell after 24 h exposure to polymersomes loaded with 15 nm gold-labelled IgG antibodies (a). Specific events such as polymersome endocytosis (PE), trafficking vesicle (TV) and the early endosome (EE) escape can be observed. The gold-labelled antibodies delivered within the cell cytosol are circled. A schematic representation of polymersome-mediated delivery of antibodies within mammalian cells (b).

Subcellular targeting

We have demonstrated that this novel methodology is comparable to a traditional immunolabelling technique in terms of signal intensity. Figures S1a and S1c show similar signal density distributions for the same antibody delivered into both live cells (by means of polymersomes) and fixed cells. Accordingly, the next step was to demonstrate that the antibody payload retained its functionality. We tested subcellular targeting of cytosolic protein targets within the cell by encapsulating antibodies targeting specific intracellular epitopes. In Figure 3a, polymersomes loaded with mouse monoclonal anti-human- α -tubulin FITC-labelled IgG (anti α -tubulin) were exposed to live HDF cells for 24 h. Tubulin filaments were positively stained to confirm the targeting and functionality of the antibodies.

This suggests that the polymersomes play a protective role during intracellular delivery as well as allowing the subsequent release of the antibody within the cell cytosol. Comparing both live and fixed specimens revealed disparities in the labelled structures. With traditional fixative techniques, paraformaldehyde crosslinks²⁴ the cytoskeleton, resulting in long tubular structures being stained. However, this effect was not observed in live samples. The α -tubulin labelling revealed shorter, more dynamic fibres. This is very much in line with the plasticity of the motile cytoskeleton of the cell²⁵.

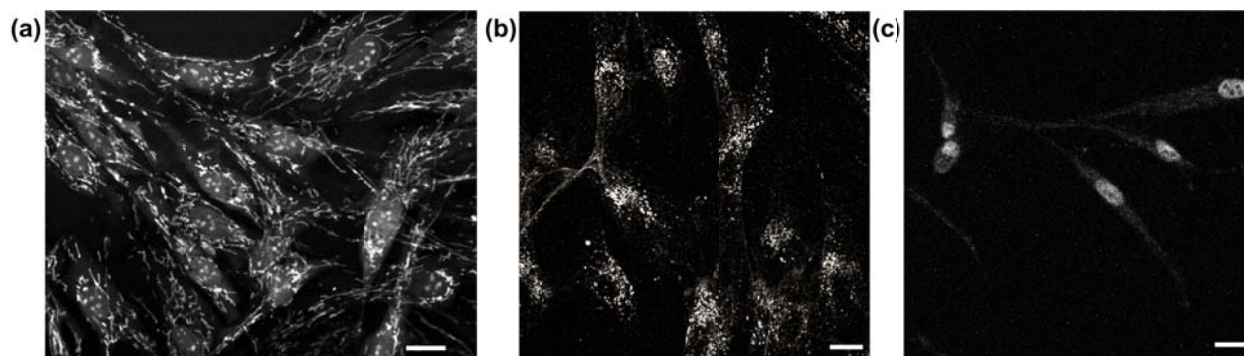


Figure 3: Distribution of internalised polymersomes encapsulating intracellular epitope-targeting antibodies. CLSM imaging of the intracellular delivery of polymersomes loaded with mouse monoclonal anti-human- α -tubulin FITC-labelled IgG into live HDF cells. Live CLSM cell imaging of the intracellular delivery of polymersomes encapsulating AlexaFluor 546-Rabbit polyclonal to human NF κ B-p65 IgG into HDF cells unstimulated (b) and stimulated with Lipopolysaccharides (LPS) (c).

Achieving live imaging of structural proteins is very useful for descriptive biology, however, the real challenge for the intracellular delivery of antibodies is the development of new tools to interrogate live cells for the study of functional proteins (such as those involved in cell signalling, stem cell differentiation, immune response or cell cycle) in their specific biological context, rather than using cell fixation techniques (as in traditional immunolabelling). On the one hand, such *in situ* studies should reveal vital mechanistic information, but perhaps more importantly modulation of the activity of these proteins might provide a new avenue for pharmacological therapies. Thus we evaluated the ability of these polymersomes to mediate intracellular delivery of antibodies to one well-known example of a functional protein: the nuclear transcriptional factor, NF- κ B.²⁶ This is an evolutionarily conserved protein complex that plays a pivotal role in the immune system by modulating the expression of inducers and effectors in response to pathogens, cellular stress, free radicals etc.²⁷ Under normal conditions, NF- κ B complexes are localized in the cytoplasm and are typically bound to a family of inhibitory proteins (I κ Bs) that are known inhibitors of NF- κ B. Upon receptor ligation and recruitment of receptor proximal adaptor proteins, a cascade of events is triggered that ultimately leads

to I κ B degradation. This exposes the NF- κ B nuclear location sequence (NLS) allowing its translocation to the nucleus.^{27, 28} When cells are not stimulated, the inactive NF- κ B is mainly located within the cell cytoplasm. As shown in Figure 3b, imaging of live non-stimulated cells treated with polymersomes loaded with a AlexaFluor 546-Rabbit polyclonal to human NF κ B-p65 IgG (anti p65) reveals a distribution of this antibody within the cell cytosol. The nuclear translocation of NF- κ B is triggered on cellular stimulation using lipopolysaccharide (LPS), hence treatment with antibody-loaded polymersomes localises the payload mainly within the nuclear region (Figure 3c).

Intracellular expression of antibodies is a non-trivial problem^{29, 30}. Antibodies are designed to be extruded through reticulum and secreted into the extracellular space within B-cells. The main challenge for the retention of these proteins inside the cytosol is the redox environment of the cytosolic compartment^{29, 30}. In principle, a system that is able to deliver already fully-functional antibodies may overcome such problems. In our work, HDF cells were incubated for 24 h with polymersomes loaded with mouse-anti human-Golgin-97 monoclonal IgG (which acts as a primary antibody). Following this treatment, cells were treated for 2 h with polymersomes encapsulating AlexaFluor 546 goat Anti-mouse IgG (which acts as a secondary antibody) to perform double immunolabelling within live cells (see Figures 4a and 4b). As an internal control, fixed HDF cells were labelled using a traditional immunolabelling technique with both antibodies (Figures 4c and 4d). Both techniques allowed similar staining of the Golgi structure to be achieved. This suggests that polymersome-mediated delivery maintains the functional structure of the antibody after intracellular release of the payload. Furthermore, the effective staining achieved using secondary and primary antibodies allows maximum flexibility in selecting the target, as well as enhancing the signal. Indeed secondary antibodies are often designed to target more than one epitope of the primary one allowing multilabelling and increased the signal to noise ratio.

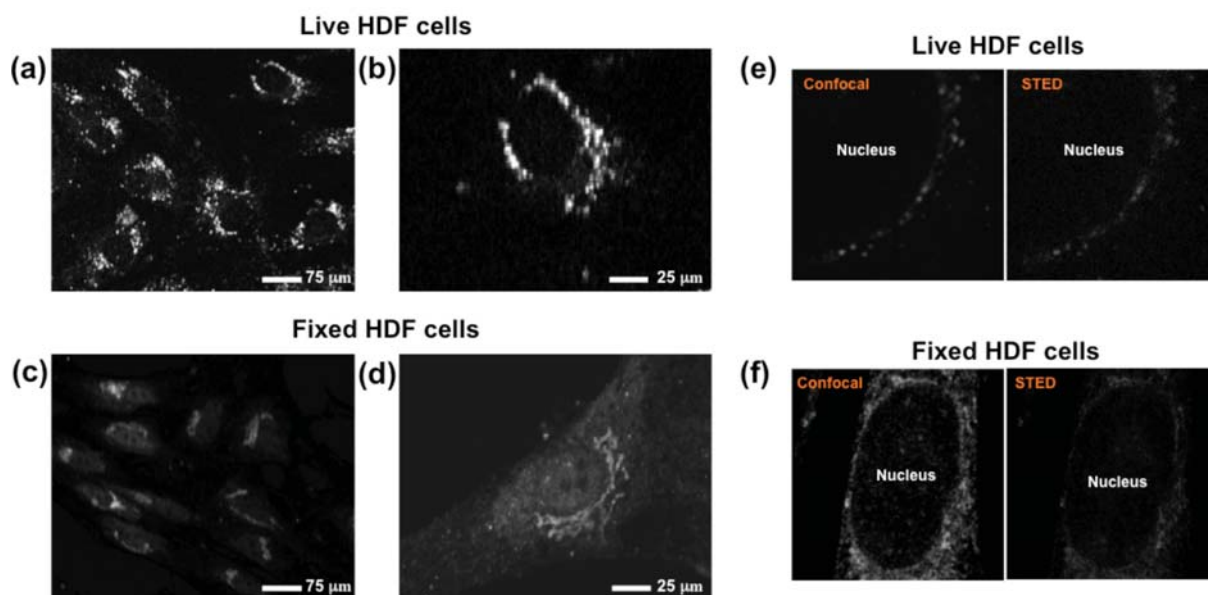


Figure 4. Double immunolabelling and STED microscopy. Live immunolabelling of Golgin-97 in HDF cells. **(a-b)** HDF cells treated with polymersomes loaded with mouse-anti human-Golgin-97 monoclonal IgG for 24 h and subsequently with AlexaFluor 546 goat Anti-human IgG for 2 h before being visualised by CLSM. **(c-d)** Conventional immunolabelling of Golgi apparatus. Confocal and STED imaging of live **(e)** and conventional **(f)** immunolabelling of nuclear protein Lamin A/C using ATTO647 dye-labelled rabbit-anti human-lamin-monoclonal IgG.

Recently, optical imaging has been revolutionised by the invention of stimulated emission depletion microscopy (STED) microscopy.³¹⁻³³ An ingenious combination of two concentric lasers allows one laser pulse to excite the specimen while the second laser pulse “depletes” the excited states of any fluorophores. This set-up enables a resolution of tens of nanometres to be achieved. STED has been used to analyse sub-cellular structures and processes in their native environment with minimal perturbation. However, STED imaging is limited to only a few dyes that have the correct photophysical characteristics to be both excited and depleted with high quantum yields.³² Herein, we have evaluated our polymersome-based technology to deliver functional antibodies within live cells using STED-optimised ATTO-647 anti human lamin IgG. As shown in Figure 4e sufficient antibodies are delivered to allow STED imaging and hence produce high resolution images of live cells that are comparable to those achieved using the traditional fixation methods (Figure 4f).

Therapeutic impact

In addition to their use as investigative tools, antibodies are of increasing interest as therapeutic agents; either in combination with drugs or as blocking agents for specific signals.³⁴ Indeed, therapeutic antibodies are one of the fastest developing areas of the biopharmaceutical industry, with total annual sales expected to exceed \$50 billion within the next few years. There are 23 therapeutic products based on monoclonal-neutralising antibodies and 3 based on antibody fragments that are currently available, with a market impact of over \$1 billion sales per year).³⁵ However, despite numerous attractive intracellular targets, antibody therapeutics have been principally restricted to the extracellular space. This is generally due to the lack of an efficient delivery vehicle for the transport of functional polypeptides within cells without inducing cytotoxicity. It appears evident that the herein proven ability to deliver functional antibodies can have a tremendous impact on designing new therapies based on *ad-hoc* engineered antibodies. To demonstrate this potential, we delivered labelled and non-labelled rabbit polyclonal to human NFκB-p65 IgG in order to target the p65 subunit of the nuclear transcription factor NF-κB. As shown in Figures 3c and 3b, the polymersome-mediated delivery of anti-p65 antibodies effectively targeted NF-κB, either when the complex is within the cytosol or in the nucleus. Furthermore, we examined whether the delivery of the anti-p65 antibody had an effect on the ability of NF-κB to translocate to the nucleus upon activation. Using CLSM (see Figure 5a) we observed that, on increasing the antibody load inside the cells, the majority of the fluorescent signal **originates** from the perinuclear area of activated cells.

This suggests that the antibody hinders the translocation of the NF-κB to the nucleus. This finding was corroborated by quantification of the NF-κB translocation via immunofluorescence as a function of the delivered antibody concentration. While either untreated cells or cells treated with empty polymersomes displayed effective translocation upon LPS stimulation, this effect is inhibited as cells are treated with increasing concentrations of antibody, with almost full inhibition being observed at the highest antibody concentrations, see Figure 5b. Due to the deficient NF-κB translocation, the profile of pro-inflammatory cytokine expression upon LPS activation was considerably reduced in HDF cells (Figures 5c and 5d). This proof-of-concept experiment demonstrates the potential therapeutic use of neutralising antibodies. Normal skin tissue contains non-hematopoietically-derived cells such as fibroblasts, keratinocytes and endothelial cells. These can produce NF-κB inducible cytokines which stimulate and recruit T-cells into the skin upon inflammation.^{36,37} In particular, human dermal fibroblasts are known to release different amounts of pro-inflammatory cytokines (IL-6, IL-8) upon LPS induced NF-κB activation.^{36,38,39} Here we use a simple example where neutralising antibodies that

hinder the translocation of NF- κ B have a clear effect (at the protein level) on the expression of pro-inflammatory cytokines. Moreover, translation of this particular example (NF- κ B targeting) in order to target many different epitopes of interest for particular biological/therapeutic purposes should be straightforward.

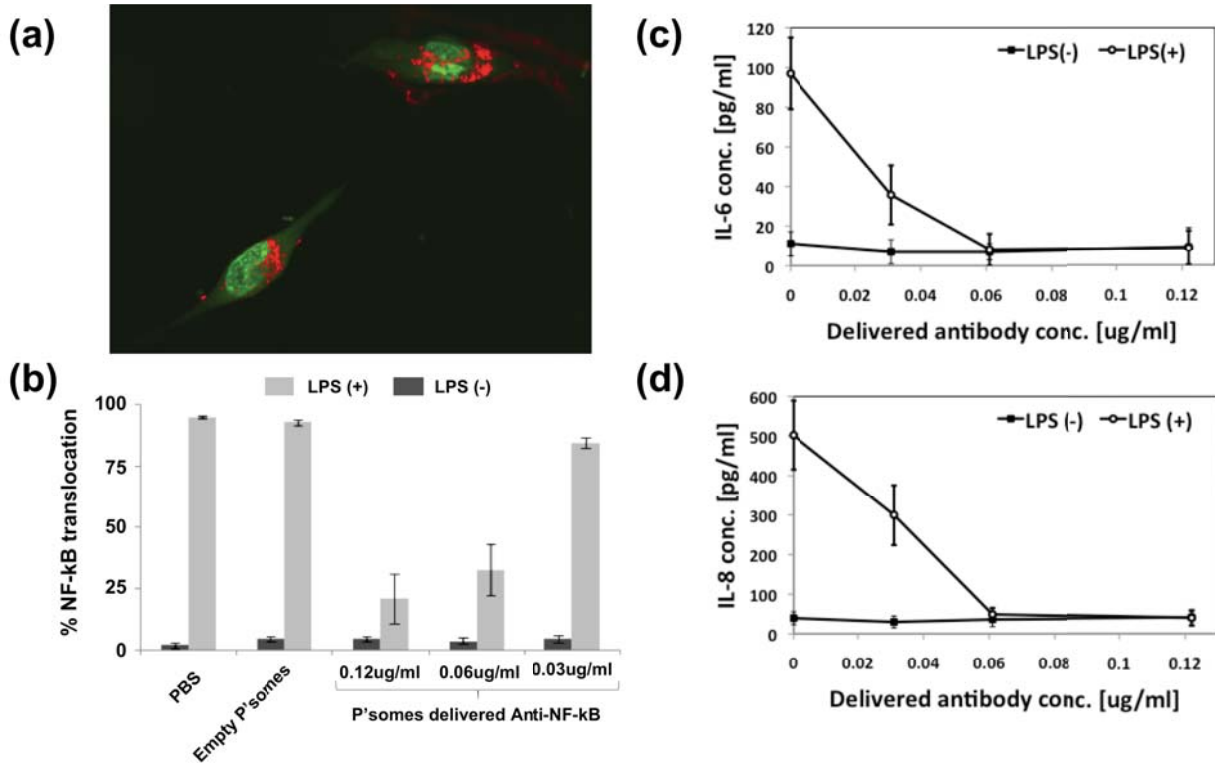


Figure 5. HDF cells after 6 h incubation with polymersomes delivered AlexaFluor546-Anti-p65-NF κ B (red) and stimulated for 2 h with 1 μ g/ml of LPS. NF- κ B accumulates around the **perinuclear** area (a). Cellular nucleic acids (DNA and RNA) were co-stained with a green SYTO9 dye. Quantification of the NF- κ B translocation (b) by immuno-labelling post stimulation of LPS (2 h) **either untreated or treated** with different concentrations of polymersomes delivering Anti-p65-NF κ B. Quantification of cytokine IL-6 (c) and IL-8 (d) release in the conditioned media of HDF cells 24 h after exposure to different concentrations of polymersomes delivering Anti-p65-NF κ B.

Discussion

We have shown that, using the appropriate polymersome-based delivery vehicle, relatively large antibodies can be efficiently delivered with retention of their functionality within live cells without inducing cellular death or stress. As the pH-sensitive polymersomes are internalised and exposed to the

acidic environment of the endosome rapid dissociation occurs, thereby promoting a local increase in the number of particles with a subsequent increase in the osmotic pressure. To overcome **this** pressure, we postulate that the excess concentration may be released outside the endosome via temporary membrane disruption, allowing delivery of the polymersome payload to the cytosol. We provide experimental evidence based on FACS, CLSM and TEM to support this hypothesis. In particular, polymersome-induced endosome destabilisation is sufficient to mediate the release of large 15 nm gold-labelled antibodies (Figure 2a). We have demonstrated the integrity of the delivered antibodies by effective intracellular epitope targeting of labelled antibodies, as judged by CLSM imaging. The data shown in Figures 3 and 4 clearly demonstrate that this approach could be used for live cell imaging, which enables immunolabelling studies of intracellular events to be conducted without the intrinsic limitations associated with cell fixation. This opens up a new window on biological research by revealing relevant intracellular details in real time and, if combined with state-of-the-art optical techniques such as STED imaging, this approach can have substantial impact on both cellular biology and biophysics.

Finally, polymersomes are known to be non-ergodic enclosed structures containing a tightly entangled membrane⁴⁰. In contrast to the more dynamic, thin-walled liposomes, the robust nature of polymersome membranes prevent leakage of the payload and thus protects the encapsulated protein from the environment⁴. We have already confirmed that polymersomes offer an excellent platform technology for the efficient delivery of various species via both topical and systemic administration.⁴¹ In particular, PMPC-PDPA polymersomes can deliver antibodies intracellularly *in vivo* with **little or** no associated toxicity **or** morbidity.⁴² In principle, the combination of effective delivery across cell membranes with state-of-the-art antibody engineering has the potential to revolutionise the treatment of many diseases.

Materials and methods

Materials. 2-(Methacryloyloxy)ethyl phosphorylcholine (MPC; > 99 %) was kindly donated by Biocompatibles UK Ltd. 2-(Diisopropylamino)ethyl methacrylate (DPA) was purchased from Scientific Polymer Products (USA). Copper(I) bromide (CuBr; 99.999 %), 2,2-bipyridine (bpy), methanol and isopropanol were purchased from Aldrich and were used as received. The silica used for removal of the ATRP copper catalyst was column chromatography grade silica gel 60 (0.063-0.200 mm) purchased from E. Merck (Darmstadt, Germany). 2-(*N*-Morpholino)ethyl 2-bromo-2-methylpropanoate (ME-Br) initiator was synthesised according to a previously reported protocol⁴³. Chloroform was purchased from Fisher Scientific, phosphate buffer saline (PBS) tablets from Oxoid Ltd, and sepharose 4B from Sigma-Aldrich. DMEM media and foetal calf serum were bought from Biosera (UK) and L-glutamine, penicillin streptomycin and Amphotericin B were bought from Sigma

(UK). Collagenase A was purchased from Boehringer-Mannheim (Lewes, UK). For the MTT-ESTA assay, 3-(4,5-dimethylthiazol-2-yl)-2,5 diphenyl tetrazolium bromide (MTT) was purchased from Sigma-Aldrich (UK) and hydrochloric acid was obtained from BDH AnalaR. Antibodies were purchased from Abcam (USA).

Copolymer synthesis The PMPC₂₅-PDPA₇₀ block copolymer was prepared by atom transfer radical polymerisation using a previously reported method.[1] Briefly, MPC was polymerised first in methanol using [MPC]:[MEBr]:[CuBr]:[bpy] = 25:1:1:2. After 2 hours the reaction reached 98 % conversion at which point a solution of DPA (70 eq) in methanol was added via cannula. After 40 h, ¹H NMR studies indicated that both monomers had been consumed. After quenching with methanol purification was carried out by dialysis against pure water for 5 days. Subsequent lyophilisation yielded the white copolymer product. Characterisation by gel permeation chromatography indicated the block copolymer was well defined with an M_n value of 23,000 gmol⁻¹ and M_w/M_n of 1.2.

Polymersome preparation and antibody encapsulation. PMPC₂₅-PDPA₇₀ copolymer (20 mg) was added to a glass vial and dissolved in a solution of 2:1 chloroform: methanol, at a concentration of 3 mg/ml. The solvent was evaporated under vacuum in sterile conditions, resulting in a copolymer film deposited on the walls of the vial. The copolymer film was rehydrated under sterile conditions using phosphate buffer saline (100 mM PBS) at pH 2 to form a 0.5 % w/w copolymer suspension. The solution was then sterilized by filtration (200 nm pore size). The solution pH was then increased to pH 6 and antibodies solution (0.025 mg/ml) was added to the vesicle dispersion, which was then sonicated for 10 minutes. Polymersomes encapsulating antibodies were purified via gel permeation chromatography (GPC), using a size exclusion column containing Sepharose 4B and using PBS at pH 7.3 to elute the vesicles. The fractions that contained polymersome encapsulating antibody, as determined by measuring the UV absorption at 546 nm using a Perkin Elmer Lambda 25 UV spectrophotometer, were used to treat the cells. Polymersomes encapsulating mouse monoclonal anti-human- α -tubulin FITC labelled IgG antibody were added of trypan blue (0.100 ml) before sonication in order to enhance the final imaging resolution. This molecule quenched the fluorescently-labeled antibodies left over within the endosome.

Cell culture. Primary human dermal fibroblasts (HDF) were isolated from skin obtained from abdominoplasty or breast reduction operations (according to local ethically approved guidelines, NHS Trust, Sheffield, UK). Primary cultures of fibroblasts were established as previously described⁴⁴. Briefly, the epidermal layer of the skin was removed by trypsinisation and the remaining dermal layer was washed in PBS. The dermis was then minced using surgical blades and incubated in 0.5 % (w/v) collagenase A at 37°C overnight in a humidified CO₂ incubator. A cellular pellet was collected from the digest and cultured in DMEM (Sigma, UK) supplemented with 10 % (v/v) foetal calf serum, 2 mM L-glutamine, 100 IU/ml penicillin, 100 mg/ml streptomycin and 0.625 μ g/ml amphotericin B. Cells were sub-cultured routinely using 0.02 % (w/v) EDTA and used for experimentation between passages 4 and 8.

Delivery of antibodies with PMPC₂₅-PDPA₇₀: Human Dermal Fibroblast (HDF) cells were seeded at a density of 1 x 10⁵ cells per well in a six-well plate (or on coverslips). Once cells achieved 80% confluence (typically within 48 h), the medium was replenished with an aqueous solution containing 0.005 mM antibody-loaded polymersome (antibody concentration = 0.03 μ M). Delivery of polymersomes encapsulating either AlexaFluor 546 goat Anti-human IgG or mouse monoclonal anti-human- α -tubulin FITC-labelled IgG was achieved by incubation for 24 h at 37 °C. Polymersomes containing AlexaFluor 546-Rabbit polyclonal to human NF κ B-p65 antibody were loaded onto HDF cells for 6 h to ensure cellular uptake (this time period was selected based on previous experiments to establish optimal cellular uptake conditions). To activate NF κ B translocation, cells were exposed to

polymersomes containing anti-p65NFκB antibody for 6 h and then stimulated with bacterial lipopolysaccharide (LPS, Sigma-Aldrich) for 2 h. As an additional negative control to establish cellular background noise during microscopy studies, cells were treated with empty polymersomes in PBS (results not shown). Polymersomes containing mouse-anti human-Golgin-97 monoclonal IgG were loaded for 24 h at 37 °C. Cells were then washed three times with PBS. Fresh media were added in addition to polymersomes containing AlexaFluor 546 goat Anti-mouse IgG. Cells were incubated with encapsulated secondary antibodies for 2 h. The cells were finally washed three times with PBS before being directly examined by CLSM using a Zeiss LSM 510M instrument.

Stimulation emission depletion microscopy (STED) and sample preparation: HeLa cells were treated overnight with polymersomes loaded with primary anti-Lamin a+c antibodies (Abcam, UK) labelled with the Atto 647N protein labelling kit (Sigma-Aldrich). Images were acquired using a Leica TCS SP5 Spectral Confocal with STED microscope (Leica Microsystems) with live cells after careful washing to remove any polymersomes that had not been internalised. Micrographs were acquired both in confocal mode and STED mode in order to confirm the higher resolution achieved in the latter case.

Release of cytokines (IL-6, IL-8) from human dermal fibroblasts.

Cytokine release was evaluated on the harvested culture supernatants of primary human dermal fibroblasts (3×10^5 cells per well) seeded in 24-well multiwell plates (Falcon Labware, Oxnard, CA) and treated with polymersomes loaded with anti-p65NFκB antibody and/or LPS. Cells were treated similarly to those described in the previous section. This time, after stimulation for 6 h using antibody-loaded polymersomes at various concentrations and/or 2 h LPS, media were changed to a serum-free medium (to avoid residual IL-8 and IL-6 being present in the serum) in order to collect 24 h-conditioned medium. IL-6, and IL-8 were measured by immunoenzymatic methods using ELISA kits obtained from R & D System Inc, Minneapolis, USA.

Immunofluorescence detection of NF-κB activation in fibroblast by epifluorescence microscopy.

Monolayers of cells were washed three times with PBS and fixed in 10 % (w/v) formalin (500 μl per well) for 1 h. Cells were then washed three times with PBS, permeabilised with 0.1 % (v/v) Triton X100 for 20 minutes, washed three times with PBS and unreactive binding sites were blocked with 5 % (w/v) dried milk powder for 1 h. Samples were again washed three times with PBS and incubated with a primary rabbit polyclonal anti-human IgG NF-κB/p65 (c-20, Santa Cruz Biotechnology Inc., CA, USA) at a titre of 1:100 (v/v) in 1 % (w/v) milk powder in PBS at 4°C for 18 h. Cells were washed three times with PBS and incubated with a biotinylated goat anti-rabbit secondary antibody at 1:1000 (v/v) (Vector Laboratories, CA, USA) in 1 % (w/v) milk powder in PBS for 1 h at room temperature. Afterwards, wells were washed three times with PBS, and then incubated with streptavidin-FITC (Vector Laboratories, CA) at 1:100 (v/v) in PBS. Finally, three further washes with PBS were conducted before cells were visualised by epifluorescence microscopy using an AXON ImageExpress system (Axon Instruments/Molecular Devices, Union City, CA, USA). Micrographs of immuno-labelled samples were recorded at $\lambda_{ex} = 495 \text{ nm}$ / $\lambda_{em} = 515 \text{ nm}$ for FITC/NF-κB/p65 visualisation and populations of cells per field of view were scored for relative activity

References

1. Ehrlich, P. Partial cell functions. *Nobel Lecture*, 304-320 (1908).
2. Shwartzman A new method for the demonstration of antigen-antibody combination. *Science*, 127-128 (1932).
3. Du, J., Tang, Y., Lewis, A.L. & Armes, S.P. pH-Sensitive Vesicles Based on a Biocompatible Zwitterionic Diblock Copolymer. *J. Am. Chem. Soc.* **127**, 17982-17983 (2005).

4. Discher, B.M. et al. Polymersomes: tough vesicles made from diblock copolymers. *Science* **284**, 1143-1146 (1999).
5. Ren H & Chu Z, M.L. Antibodies targeting hepatoma-derived growth factor as a novel strategy in treating lung cancer. *Mol Cancer Ther* **8**, 1106-1112 (2009).
6. Biocca, A.C.a.S. Intracellular Antibodies: Development and Applications. **Springer Verlag 1997** (1997).
7. Thompson WS, G.R. Antibodies introduced into living cells with liposomes localize specifically and inhibit specific intracellular processes. . *Gene Anal Tech* **5**, 73-79 (1988).
8. Michela Visintin, Teresa Melchionna & Cattaneo, I.C.a.A. In vivo selection of intrabodies specifically targeting protein–protein interactions: A general platform for an “undruggable” class of disease targets. *Journal of Biotechnology* **135**, 1-15 (2008).
9. Curiel, D.T., Agarwal, S., Wagner, E. & Cotten, M. Adenovirus enhancement of transferrin–polylysine-mediated gene delivery. *Proc. Natl. Acad. Sci. USA* **88**, 8850-8854 (1991).
10. Cristiano, R.J., Smith, L.C., Kay, M.A., Brinkley, B.R. & Woo, S.L.C. Hepatic gene therapy: efficient gene delivery and expression in primary hepatocytes utilizing a conjugated adenovirus–DNA complex. *Proc. Natl. Acad. Sci. USA* **90**, 11548–11552. (1993).
11. Batra, R.K., Wang-Johanning, F., Wagner, E., Garver, R.I. & Curiel, D.T. Receptor-mediated gene delivery employing lectin-binding specificity. *Gene Ther* **1**, 255-160 (1994).
12. Kondo Y et al. Efficient delivery of antibody into living cells using a novel HVJ envelope vector system. *J Immunol Methods* **332**, 7-10 (2008).
13. Furusawa, M. Cellular microinjection by cell fusion: technique and applications in biology and medicine. *Int Rev Cytol* **62**, 29-67 (1980).
14. Neumann E & Schaefer-Ridder M, W.Y., Hofschneider PH. Gene transfer into mouse lyoma cells by electroporation in high electric fields. *EMBO J.* **1**, 841-845 (1982).
15. Van Tendeloo, V. et al. Highly efficient delivery by mRNA electroporation in human hematopoietic cells: superiority to lipofection and passive pulsing of mRNA and to electroporation of plasmid cDNA for tumor antigen loading of dendritic cells. *Blood* **98**, 49–56 (2001).
16. Chalfie, M., Yuan Tu, G.E., Ward, W.W. & Prasherf, D.C. Green Fluorescent Protein as a Marker for Gene Expression. *Science* **263**, 802-805 (1994).
17. Giacomelli, C., Men, L.L., Borsali, R., Armes, S.P. & Lewis, A.L. Phosphorylcholine-Based pH-Responsive Diblock Copolymer Micelles as Drug Delivery Vehicles: Light Scattering, Electron Microscopy, and Fluorescence Experiments. *Biomacromolecules* **7**, 817-828 (2006).
18. Massignani, M. et al. Controlling Cellular Uptake by Surface Chemistry, Size, and Surface Topology at the Nanoscale. *Small* **5**, 2424-2432 (2009).
19. Lomas, H. et al. Biomimetic pH Sensitive Polymersomes for Efficient DNA Encapsulation and Delivery. *Adv. Mater.* **19**, 4238-4243 (2007).
20. Massignani, M. et al. Enhanced fluorescence imaging of live cells by effective cytosolic delivery of probes. *PLoS One in the press* (2010).
21. Lomas, H. et al. Non-cytotoxic polymer vesicles for rapid and efficient intracellular delivery. *Faraday Discussions* **139**, 143-159 (2008).
22. Blanz, A., Massignani, M., Battaglia, G., Armes, S.P. & Ryan, A.J. Tailoring Macromolecular Expression at Polymersome Surfaces. *Adv. Functional Mater.* **19**, 2906-2914 (2009).
23. Massignani, M. et al. Controlling cellular uptake by surface chemistry, size, and surface topology at the nanoscale. *Small* **5**, 2424-2432 (2009).
24. Barisas, B., Wade, W., Jovin, T., Arndt-Jovin, D. & Roess, D. Dynamics of molecules involved in antigen presentation: effects of fixation. *Mol Immunol* **36**, 701-708. (1999).

25. Wang, Y., Shyy, J.Y.-J. & Chien, S. Fluorescence Proteins, Live-Cell Imaging, and Mechanobiology: Seeing Is Believing. *Annual Review of Biomedical Engineering* **10**, 1-38 (2008).
26. Baldwin, A.S. the NF-kappa B and I kappa B proteins: new discoveries and insights. *Ann. Rev. Immunol.* **14**, 649-683 (1996).
27. Hayden, M.S. & Ghosh, S. Shared principles in NF-kappaB signaling. *Cell* **132**, 344-362 (2008).
28. Perkins, N.D. Integrating cell-signalling pathways with NF-kappaB and IKK function. *Nat Rev Mol Cell Biol* **8**, 49-62 (2007).
29. Wirtz, P. & Steipe, B. Intrabody construction and expression III: engineering hyperstable V(H) domains. *Protein Sci* **8**, 2245-2250 (1999).
30. Biocca, S., Ruberti, F., Tafani, M., Pierandrei-Amaldi, P. & Cattaneo, A. Redox state of single chain Fv fragments targeted to the endoplasmic reticulum, cytosol and mitochondria. *Biotechnology (N Y)* **13**, 1110-1115 (1995).
31. Hell, S.W. Toward fluorescence nanoscopy. *Nature Biotechnol.* **21**, 1347-1355 (2003).
32. Hell, S.W. Far-Field Optical Nanoscopy. *Science* **316**, 1153-1158 (2007).
33. Hell, S.W. & Wichmann, J. Breaking the diffraction resolution limit by stimulated emission: Stimulated emission depletion microscopy. *Opt. Lett.* **19**, 780-782 (1994).
34. Nelson, A.L. & Reichert, J.M. Development trends for therapeutic antibody fragments. *Nature Biotech.* **27**, 331-337 (2009).
35. Sidhu, S.S. & Fellouse, F.A. Synthetic therapeutic antibodies. *Nat Chem Biol* **2**, 682-688 (2006).
36. Perfetto B, Donnarumma G, Criscuolo D, Paoletti I, Grimaldi E, Tufano MA, Baroni A. Bacterial components induce cytokine and intercellular adhesion molecules-1 and activate transcription factors in dermal fibroblasts. *Res Microbiol.* **154** (5) :337-44 (2003).
37. Bell S, Degitz K, Quirling M, Jilg N, Page S, Brand K. Involvement of NF-kappaB signalling in skin physiology and disease. *Cell Signal.* **15** (1):1-7 (2003).
38. Divergent gene regulation and growth effects by NF-kappa B in epithelial and mesenchymal cells of human skin. Hinata K, Gervin AM, Jennifer Zhang Y, Khavari PA. *Oncogene* **3** ;22 (13):1955-64 (2003).
39. Andreakos E, Smith C, Kiriakidis S, Monaco C, de Martin R, Brennan FM, Paleolog E, Feldmann M, Foxwell BM. Heterogeneous requirement of IkappaB kinase 2 for inflammatory cytokine and matrix metalloproteinase production in rheumatoid arthritis: implications for therapy. *Arthritis Rheum.* **48** (7):1901-12 (2003).
40. Battaglia, G. & Ryan, A.J. Bilayers and Interdigitation in Block Copolymer Vesicles. *J. Am. Chem. Soc.* **127**, 8757-8764 (2005).
41. LoPresti, C., Lomas, H., Massignani, M., Smart, T. & Battaglia, G. Polymersomes: nature inspired nanometer sized compartments. *Journal of Materials Chemistry* **19**, 3576-3590 (2009).
42. Murdoch, C. et al. Internalization and biodistribution of polymersomes into oral squamous cell carcinoma cells in vitro and in vivo. *Nanomedicine in the press* (2010).
43. Robinson, K.L., Weaver, J.V.M., Armes, S.P., Marti, E.D. & Meldrum, F.C. Synthesis of controlled-structure sulfate-based copolymers via atom transfer radical polymerisation and their use as crystal habit modifiers for BaSO₄. *J. Mater. Chem.* **12**, 890-896 (2002).
44. Chakrabarty, K.H. et al. Development of autologous human epidermal/dermal composites based on sterilised human allodermis for clinical use. *Brit J Dermatol.* **141**, 811-823 (1999).

Supplementary information

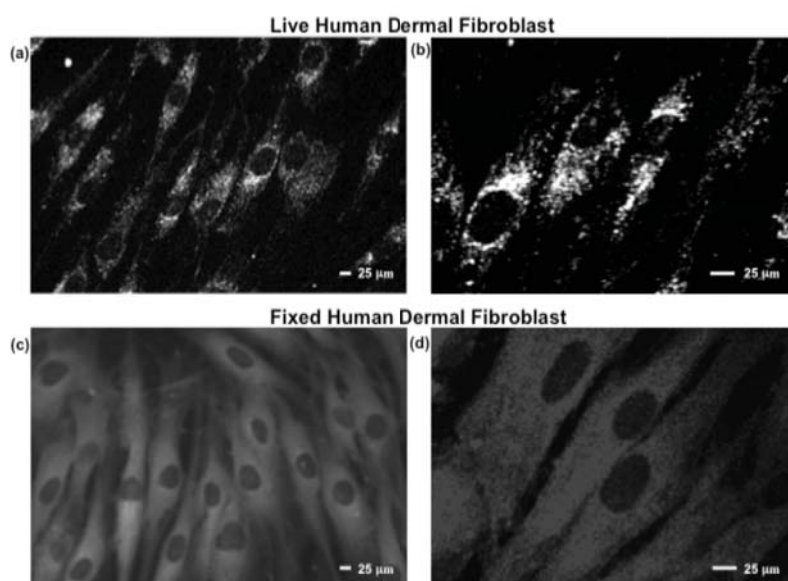


Figure S1: HDF cells were cultured in the presence of AlexaFluor 546 goat Anti-mouse IgG-loaded polymersomes. Intracellular delivery of antibodies was studied by confocal laser scanning microscopy (CLSM). (a) Live CLSM cell imaging of intracellular delivery of polymersomes encapsulating AlexaFluor 546 goat Anti-mouse IgG into live HDF cells; (b) a higher magnification image of (a) (x 3); (c) fixed CLSM cell imaging by traditional immunolabelling of HDF cells using AlexaFluor 546 goat Anti-mouse IgG; (d) a higher magnification image of (c)

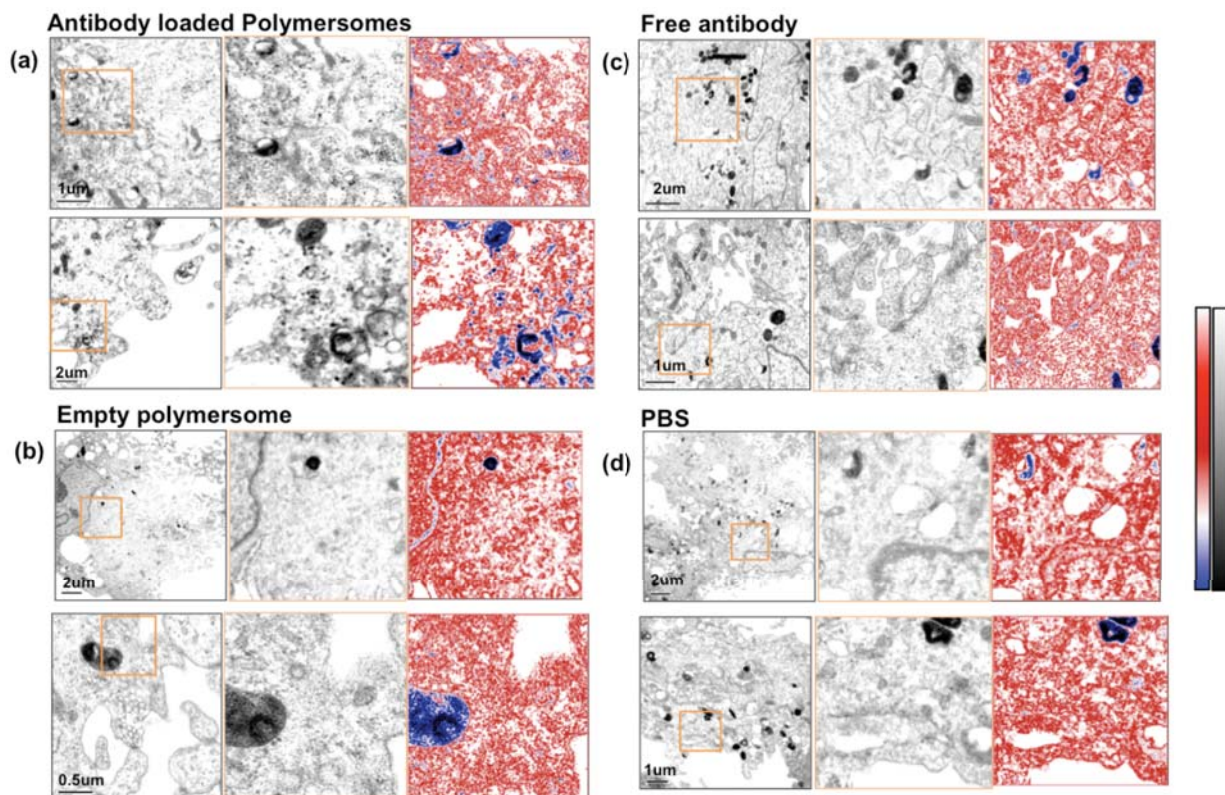


Figure S2: TEM images showing sections of HDF cells obtained at different magnifications after incubation with 15 nm gold-labelled antibody-loaded polymersomes, free antibodies, empty polymersomes and PBS. It is evident that the gold-labelled antibodies are visible within the cell cytosol only when delivered using the polymersomes. Cell were imaged in two different area, the magnification are also displayed using a color gradient to highlight the dense gold antibodies.